On LES of low-speed flows by high-order shock-capturing schemes with flow sensors

By D. Kotov, H.C. Yee †, A. Wray † AND B. Sjögreen ‡

1. Introduction

For the last decade, high-order shock-capturing methods with numerical dissipation controls have been the state-of-the-art numerical approach for direct numerical simulation (DNS) and large eddy simulation (LES) of turbulent flows with shocks. See, for example Yee & Sjögreen (2010, 2007); Sjögreen & Yee (2004); Yee *et al.* (1999, 2012); Kotov *et al.* (2013, 2014); Lombardini *et al.* (2011); Johnsen *et al.* (2010); Touber & Sandham (2011); Lo *et al.* (2010). The majority of these methods involve flow sensors with parameter tuning applied depending on the flow type. Some of the flow sensors were designed for certain flow types and might not preserve their high accuracy when used to simulate a flow of a different type. In a study presented in Johnsen *et al.* (2010), all of the shock-capturing schemes involve tuning of the parameters. It appears that the Yee & Sjogreen filter scheme is not as accurate as the hybrid scheme presented in Johnsen *et al.* (2010) because the key parameter κ responsible for minimizing the numerical dissipation in the scheme of Yee & Sjögreen (2007) was set to a constant based on the initial flow Mach number. See (Yee & Sjögreen 2010; Kotov *et al.* 2013) for a description of better control of numerical dissipation using a local κ. The hybrid scheme presented in Johnsen *et al.* (2010) which employed the flow sensor of Ducros *et al.* (1999) also consists of a key tuning parameter δ. From our study presented below of the same Taylor-Green vortex problem considered in Johnsen *et al.* (2010), the cut-off parameter δ is set 1 to achieve the best accurate result. On the other hand, for the isotropic turbulence with shocklets test case, the Ducros et al. flow sensor δ parameter has to be greatly reduced, mostly by trial and error. Yet in another study (Kotov *et al.* 2014) for turbulence interacting with a high speed stationary shock, depending on the Mach number and turbulent Mach number, different values of δ are required for each case.

In recognizing the different requirements on numerical dissipation control for DNS and LES of a variety of compressible flow types, Yee & Sjögreen (2010) presented a general framework for a local κ, and the accompanying variety of flow sensors were introduced into their high-order nonlinear filter scheme. Aside from suggesting different local κ formulation, Yee & Sjogreen also proposed the use of a combination of different flow sensors. Their proposed scheme with numerical dissipation control has not been studied extensively. A subset to the sequel to Yee & Sjögreen (2010) was presented in Yee *et al.* (2011); Kotov *et al.* (2013). This is yet another sequel to Yee & Sjogreen. The goal of this work is to examine the different combinations of flow sensors for DNS and LES of low-speed turbulent flows. For the LES numerical experiments, two low-speed flows are considered: (a) The 3D compressible viscous counterpart of the very low-speed shock-free turbulence Taylor-Green vortex problem considered in Johnsen *et al.* (2010) and (b) the same isotropic turbulence with shocklets as in Johnsen *et al.* (2010).

† NASA Ames Research Center
‡ Lawrence Livermore National Laboratory

2. Governing equations and SGS models

We consider the governing equations written as

$$\partial_t \bar{\rho} + \partial_j(\bar{\rho}\tilde{u_j}) = 0, \tag{2.1}$$

$$\partial_t(\bar{\rho}\tilde{u_i}) + \partial_j(\bar{\rho}\tilde{u_i}\tilde{u_j} + \bar{p}\delta_{ij} - \check{\tau}_{ij} + \tau^S_{ij}) = 0, \tag{2.2}$$

$$\partial_t(\bar{\rho}\tilde{E}) + \partial_j(\bar{\rho}\tilde{E}\tilde{u_j} + \bar{p}\tilde{u_j} - \check{\tau}_{ij}\tilde{u_i} + \check{q}_j + q^S_j) = 0, \tag{2.3}$$

where ρ is density, u_i is i^{th} velocity component, p is the pressure, T is the temperature, E is the total Energy, and t is the time. For given f, LES filtering operation is denoted as $\bar{f}$. Favre filtering operation is denoted as $\tilde{f} = \overline{\rho f}/\bar{\rho}$, and $\check{f}$ stands for the function of the Favre-filtered variables introduces as

$$\check{\tau}_{ij} = 2\mu(\tilde{T})(\tilde{S}_{ij} - \frac{1}{3}\delta_{ij}\partial_k\tilde{u}_k), \quad \tilde{S}_{ij} = (\partial_j\tilde{u}_i + \partial_i\tilde{u}_j)/2, \quad \check{q}_j = -\lambda(\tilde{T})\partial_j\tilde{T}, \tag{2.4}$$

where dynamic viscosity is given by $\mu(T) = \mu_0(T/T_0)^{3/4}$ and thermal conductivity is expressed through a constant Prandtl number Pr and heat capacity at constant pressure c_p ($\lambda(T) = c_p\mu(T)/Pr$). The equation of state is $\bar{p} = R\bar{\rho}\tilde{T}$, where R is the gas-specific constant. The subgrid-scale (SGS) terms, SGS stress tensor τ^S_{ij} and SGS heat flux q^S_j, are modeled as

$$\tau^S_{ij} - \frac{1}{3}\tau^S_{kk}\delta_{ij} = -2\mu_t(\tilde{S}_{ij} - \frac{1}{3}\tilde{S}_{kk}\delta_{ij}), \quad \tau^S_{kk} = 2C_I\bar{\rho}\Delta^2|\tilde{S}|^2, \quad q^S_j = \frac{\mu_t\gamma c_v}{Pr_t}\partial_j\tilde{T}, \tag{2.5}$$

where $\mu_t = \bar{\rho}C_s\Delta^2|\tilde{S}|$, $|\tilde{S}| = \sqrt{2\tilde{S}_{ij}\tilde{S}_{ij}}$ and Δ is the filter width. Note that for the current study we use implicit filtering in Eqs. (2.1-2.3), with the filter width determined by the grid spacing. LES with explicit filtering will be considered in future studies.

In the Smagorinsky model, C_s is defined as a problem-specific constant. In this study we use $C_s = 0.0085$ (Erlebacher *et al.* 1992). Simulations using this model are denoted as LES1.

In the dynamic SGS model, the Smagorinsky constant C_s and the constant for the isotropic part of the SGS stress C_I are obtained through the Germano-Lilly (Germano *et al.* 1991; Lilly 1992) procedure, which can be written as

$$C_s = \frac{\left\langle L^{C_s}_{ij} M^{C_s}_{ij} \right\rangle_H}{\left\langle M^{C_s}_{ij} M^{C_s}_{ij} \right\rangle_H}, \qquad C_I = \frac{\langle L_{ll} \rangle_H}{\left\langle M^{C_I}_{ll} \right\rangle_H}, \tag{2.6}$$

where

$$L^{C_s}_{ij} = L_{ij} - \frac{1}{3}L_{ll}\delta_{ij}, \qquad L_{ij} = \left(\bar{\rho}\widehat{\tilde{u}_i\tilde{u}_i}\right) - \hat{\bar{\rho}}\hat{\tilde{u}}_i\hat{\bar{\rho}}\hat{\tilde{u}}_i/\hat{\bar{\rho}}, \tag{2.7}$$

$$M^{C_s}_{ij} = -2\hat{\bar{\rho}}\hat{\Delta}^2|\hat{\tilde{S}}|^2\left(\tilde{S}_{ij} - \widehat{\frac{1}{3}\tilde{S}_{ll}\delta_{ij}}\right) + 2\Delta^2\left[\left(\bar{\rho}|\tilde{S}|\widehat{\tilde{S}_{ij}}\right) - \frac{1}{3}\left(\bar{\rho}|\tilde{S}|\widehat{\tilde{S}_{ll}}\delta_{ij}\right)\right], \tag{2.8}$$

$$M^{C_I}_{ll} = 2\hat{\bar{\rho}}\hat{\Delta}^2|\hat{\tilde{S}}|^2 - 2\Delta^2\left(\bar{\rho}|\tilde{S}|^2\right), \tag{2.9}$$

and $< f >_H$ stands for averaging in homogeneous directions. The Germano procedure requires an explicit filtering operation, denoted here with the top hat symbol. For this filtering operation we use a 3D operator based on 1D trapezoidal filter discretized as

$$\hat{f}_i = \frac{1}{4}f_{i-1} + \frac{1}{2}f_i + \frac{1}{4}f_{i+1}. \tag{2.10}$$

Simulations using this dynamic SGS model are denoted as LES2.

For the cases with low turbulent Mach number $M_t < 0.4$, it is shown (Erlebacher *et al.* 1992) that the isotropic part of the SGS stress can be neglected ($C_I = 0$). Early numerical experiments comparing the case of setting $C_I = 0$ vs. the non-zero case produced a similar result by the LES1 model for a 3D isotropic turbulence test case using a $M_{t,0} = 0.6$ (Johnsen *et al.* 2010). There is, however, a slightly different result from the LES2 on some of the computed flow quantities by using the non-zero C_I. Only results using $C_I = 0$ will be presented for the same isotropic turbulence test case in the later section.

3. Test cases

This section illustrates the performance of our high-order filter scheme for DNS and LES of two 3D low-speed turbulence flows considered in Johnsen *et al.* (2010). The first test case is the nearly incompressible (inviscid) Taylor-Green vortex problem and its viscous counterpart. The second test case is the decay of an isotropic turbulence with shocklets for an initial turbulent Mach number $M_{t,0} = 0.6$. For both test cases grid convergence studies are performed using uniform 256^3, 128^3 and 64^3 grids for the DNS simulations. Grid convergence studies also are performed using uniform 128^3, 64^3 and 32^3 grids for LES computations. Studies found that for an accurate numerical dissipation control scheme, a coarse grid DNS using a uniform 64^3 grid compared well with the filtered DNS using a fine grid of 256^3 grid points (spectrally filtered to a 64^3 grid). For the LES computations, the 32^3 grid is too coarse for obtaining an accurate solution, whereas the 128^3 grid solutions are almost on top of the filtered DNS computation on the 256^3 grid. Here, only the results using the 64^3 are shown.

3.1. *Taylor-Green vortex*

The first test case is the 3D Taylor-Green vortex (Taylor & Green 1937) inviscid flow. The 3D Euler equations are solved with gas constant $\gamma = 5/3$. The computational domain is a 2π square cube using a uniform 64^3 grid. Boundary conditions are periodic in all directions.

The initial conditions are

$$\begin{aligned} &\rho = 1, \quad p = 100 + ([\cos(2z) + 2][\cos(2x) + \cos(2y)] - 2)/16, \\ &u_x = \sin x \cos y \cos z, \quad u_y = -\cos x \sin y \cos z, \quad u_z = 0. \end{aligned} \tag{3.1}$$

The initial turbulent Mach number is $M_{t,0} = 0.042$ and the final time is $t = 10$. We also consider the viscous counterpart of the Taylor-Green vortex problem. In the viscous case the physical viscosity is assumed to follow a power law written as

$$\mu/\mu_{ref} = (T/T_{ref})^{3/4}. \tag{3.2}$$

Here we use $\mu_{ref} = 0.005$ and $T_{ref} = 1$ in non-dimensional units. The initial Reynolds number is $Re_0 = 2040$. For this low-Mach number flow without high shear regime, the simulation actually does not require any numerical dissipation. However, we use the same shock-capturing scheme with adaptive numerical dissipation control to demonstrate its accurate performance for such low-Mach number cases. The key study involves the assessment of accuracy of the computed solution using different forms of $\kappa^l_{j+1/2}$ and different values of δ mentioned above.

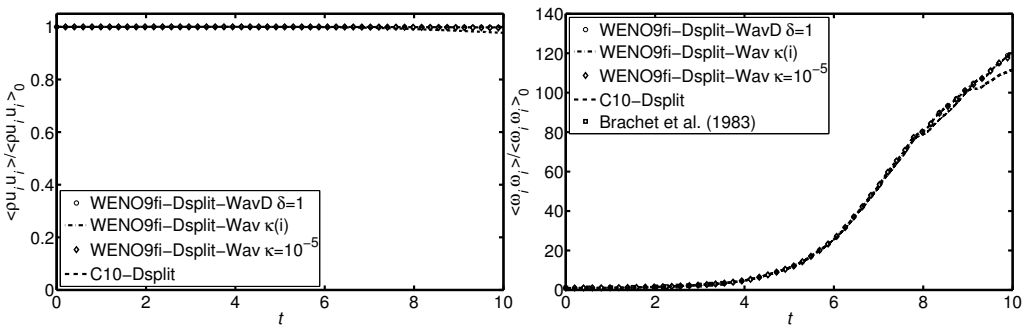

FIGURE 1. Coarse grid DNS scheme comparison for the inviscid Taylor-Green vortex problem using a 64^3 grid: Temporal evolution of the kinetic energy (left) and enstrophy (right).

3.1.1. *Inviscid case – DNS scheme comparison*

In the inviscid case the kinetic energy should be constant. It can be used as a criterion to judge the accuracy of the four considered filter numerical fluxes. The coarse grid DNS (64^3 grid – no SGS model) comparison among different methods is shown in Figure 1. Figure 1 shows the temporal evolution of the mean kinetic energy and enstrophy compared to the 256^3 grid filtered DNS reference solution. The preservation of kinetic energy is achieved with C10-split, WENO9fi-Dsplit-WavD and WENO9fi-Dsplit-Wav $\kappa = 10^{-5}$, while WENO9fi-Dsplit-Wav $\kappa(i)$ obtains a small loss in energy after $t \approx 6$. All four methods presented on the enstrophy plot demonstrate good agreement with the semi-analytical solution of Brachet *et al.* (1983), which is defined on the interval $0 \leq t \leq 3.5$. The enstrophy values obtained using WENO9fi-Dsplit-Wav $\kappa(i)$ are slightly smaller than those obtained using the other three methods.

3.1.2. *Viscous case – DNS and LES scheme comparison*

The temporal evolution of the mean-square velocity and enstrophy of the coarse grid DNS (no SGS model) results on a 64^3 grid by different methods are shown in Figure 2. The reference solution is the DNS simulation using a 256^3 grid and spectral filtering to the 64^3 grid. For this viscous case the most accurate cut-off parameter δ in WENO9fi-Esplit-WavD and WENO9fi-Dsplit-Ducr is when $\delta = 1$. The kinetic energy computed solutions by all considered methods matches the reference solution. The difference between methods is only visible on the enstrophy comparison, though all the results are very close to the reference solution. The methods using Ducros et al. split C10-Dsplit and WENO9fi-Dsplit-Wav $\kappa = 10^{-5}$ as well as WENO9fi-Esplit-Wav $\kappa(i)$ obtain slightly more accurate results than C10-Esplit and WENO9fi-Esplit-WavD.

The results obtained using the two LES models are shown in Figures 3 and 4. As observed also in the isotropic turbulence simulations (to be shown later), the results obtained in LES1 are closer to the reference solution than the results obtained using the dynamic model LES2. All LES methods underestimate both the kinetic energy and the enstrophy. WENO9fi-Esplit-Wav $\kappa(i)$ is slightly less accurate than C10-Dsplit and WENO9fi-Esplit-WavD. The accuracy by C10-Esplit and C10-Dsplit are almost the same.

3.2. *Compressible isotropic turbulence*

The second test case is the decaying compressible isotropic turbulence with eddy shocklets (Lee *et al.* 1991; Johnsen *et al.* 2010). For high enough turbulent Mach number, M_t weak shock waves (shocklets) develop spontaneously from the turbulent motions. For the

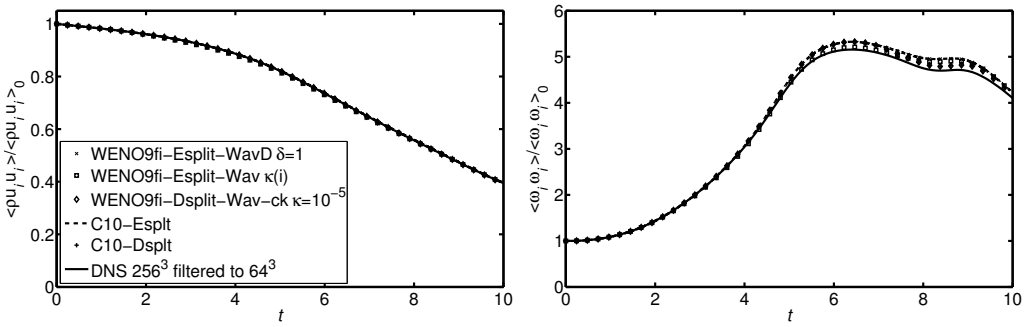

FIGURE 2. Coarse grid DNS scheme comparison for the viscous Taylor-Green vortex problem using a 64^3 grid: Temporal evolution of the kinetic energy (left) and enstrophy (right). The reference solution is the DNS computation on a 256^3 grid and spectrally filtered to a 64^3 grid.

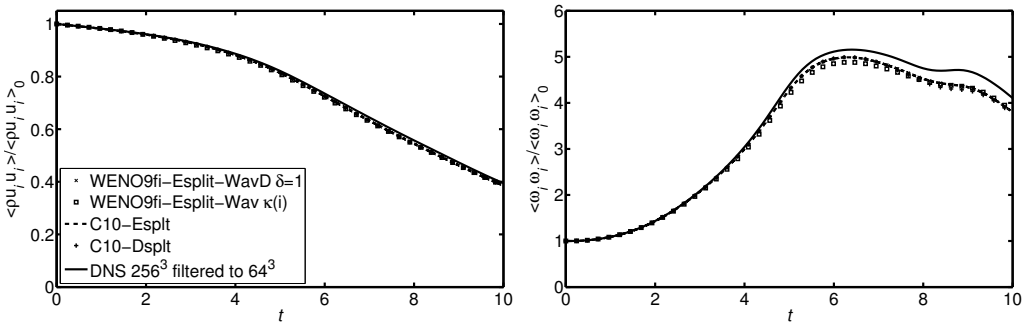

FIGURE 3. LES1 scheme comparison for the viscous Taylor-Green vortex problem using a 64^3 grid: Same as Figure 2 with the results obtained using the Smagorinsky SGS model (LES1).

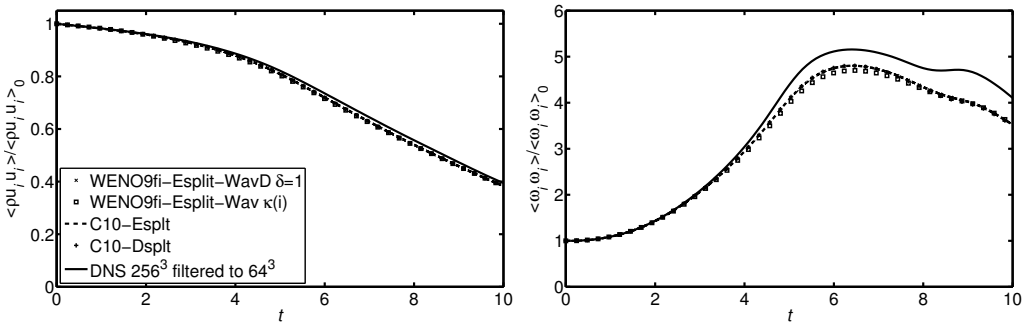

FIGURE 4. LES2 scheme comparison for the viscous Taylor-Green vortex problem using a 64^3 grid: Same as Figure 2 with the results obtained using the Germano-Lilly SGS model (LES2).

current numerical experiment we set the initial $M_{t,0} = 0.6$. The Navier-Stokes governing equations and the filtered governing equations (2.1-2.3) are solved using $\gamma = 1.4$. The computational domain is on the $2\pi^3$ cube with periodic boundary conditions in all directions. The physical viscosity is assumed to follow a power law (3.2).

The initial condition consists of a random solenoidal velocity field $u_{i,0}$ that satisfies

$$E(k) \sim k^4 \exp(-2(k/k_0)^2), \quad \frac{3}{2}u_{rms,0}^2 = \frac{\langle u_{i,0}u_{i,0}\rangle}{2} = \int_0^\infty E(k)dk. \tag{3.3}$$

The brackets here denote averaging over the entire computational domain. For this study we put $u_{rms,0} = 1$ and $k_0 = 4$. The density and pressure fields are initially constant with initial turbulent Mach number $M_{t,0} = 0.6$ and Taylor-scale Reynolds $Re_{\lambda,0} = 100$. These parameters are defined as follows:

$$M_t = \frac{\sqrt{\langle u_i u_i \rangle}}{\langle c \rangle}, \quad Re_\lambda = \frac{\langle \rho \rangle \, u_{rms} \lambda}{\langle \mu \rangle}, u_{rms} = \sqrt{\frac{\langle u_i u_i \rangle}{3}}, \quad \lambda = \sqrt{\frac{\langle u_x^2 \rangle}{\langle (\partial_x u_x)^2 \rangle}}. \tag{3.4}$$

The time scale is $\tau = \lambda_0 / u_{rms,0}$ and the final time is $t/\tau = 4$. The final turbulent Mach number is $M_t = 0.29$.

Similar to the Taylor-Green vortex problem, different values of κ and δ parameters are examined. Unlike the Taylor-Green vortex case, the most accurate solutions are obtained using a smaller κ and for values of δ between 0.7 and 1.

Comparisons of the temporal evolutions of the mean-square velocity, enstrophy, temperature variance and dilatation using the various filter numerical fluxes on a 64^3 coarse grid DNS (no SGS model) are shown in Figure 5. The reference solution was obtained from the DNS simulation using a 256^3 grid and spectral filtering to a 64^3 grid (digitized from Johnsen *et al.* (2010)). The best results are obtained with C10-AV12, WENO9fi-Dsplit-Wav $\kappa(i)$ and WENO9fi-Esplit-Ducr. The cut-off parameter of the Ducros et al. sensor in WENO9fi-Esplit-WavD is $\delta = 0.7$. However, the results remain almost the same when δ increases slightly beyond 0.7. For the dilatation, the best match with the reference solution is obtained by method C10-AV12. However, this scheme underestimates the enstrophy, while the rest of the methods either match or slightly overestimate the enstrophy.

The results obtained using the two LES models are shown in Figures 6 and 7. The LES1 computations are closer to the reference solution than the dynamic model LES2. The best results in both cases are obtained with C10-Esplit, WENO9fi-Esplit-Ducr and WENO9fi-Esplit-WavD. All presented methods in LES1 and LES2 underestimate the enstrophy and kinetic energy. The spectra of this isotropic decaying turbulence test case were examined, the computed spectra by these schemes are as expected, and results are not shown due to a space limitation.

4. Conclusions

The performance of the filter scheme with different flow sensors was demonstrated in LES and DNS of low-speed flows. Forms (1) - (4) for the filter numerical flux were chosen to demonstrate that for low-speed turbulence flows without strong shear waves, the constant κ vs. the local $\kappa^l_{j+1/2}$ behave similarly. The main difference when using the constant κ parameter is that one has to know the flow structure of the entire evolution a priori in order to select the proper constant κ parameter. Contrary to the considered low-speed flow test cases, our previous investigations (Yee *et al.* 1999; Sandham *et al.* 2002; Sjögreen & Yee 2004; Yee & Sjögreen 2007; Yee *et al.* 2012; Hadjadj *et al.* 2012; Yee & Sjögreen 2010; Kotov *et al.* 2013) for various complex high speed shock-turbulence interaction flows, employing the local $\kappa^l_{j+1/2}$ would provide an automatic selection of the amount of numerical dissipation needed at each flow location, thus leading to a more accurate DNS and LES simulation with less tuning of parameters.

Overall, the LES1 (Smagorinsky) results are closer to the filtered DNS reference solution than the LES2 (dynamic Germano) results. For the isotropic turbulence with shocklets test case using the LES1 model, the results using non-zero C_I formula indi-

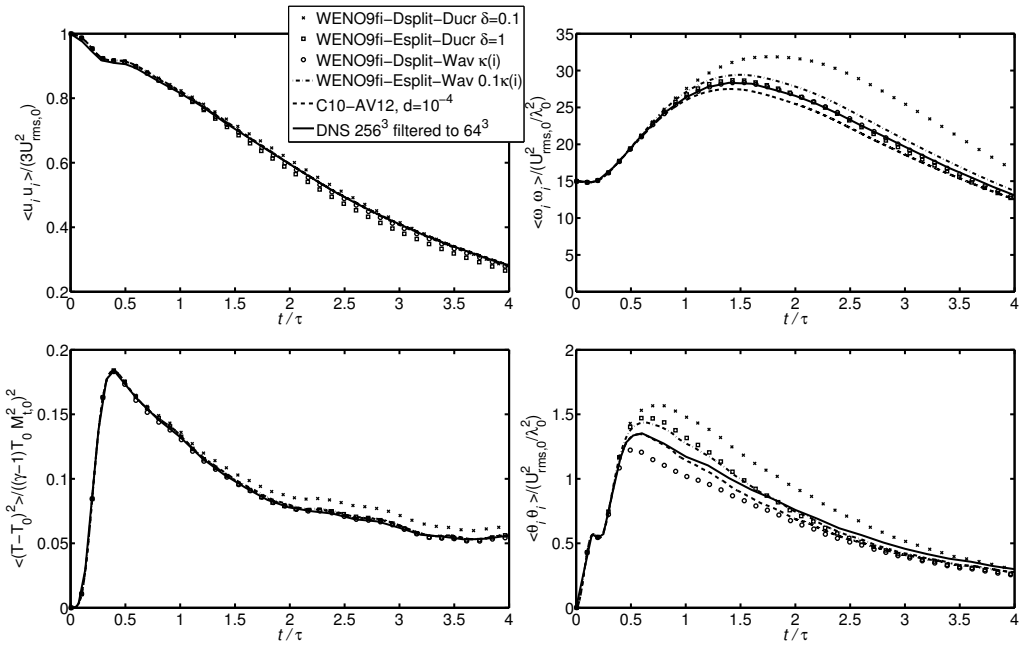

FIGURE 5. Coarse grid DNS scheme comparison for the isotropic turbulence problem using a 64^3 grid: Temporal evolution of kinetic energy (top left), enstrophy (top right), temperature variance (bottom left) and dilatation, $\theta_i = \partial_i u_i$ (bottom right). The reference is the digitized solution from Johnsen *et al.* (2010) on a 256^3 grid spectrally filtered to a 64^3 grid.

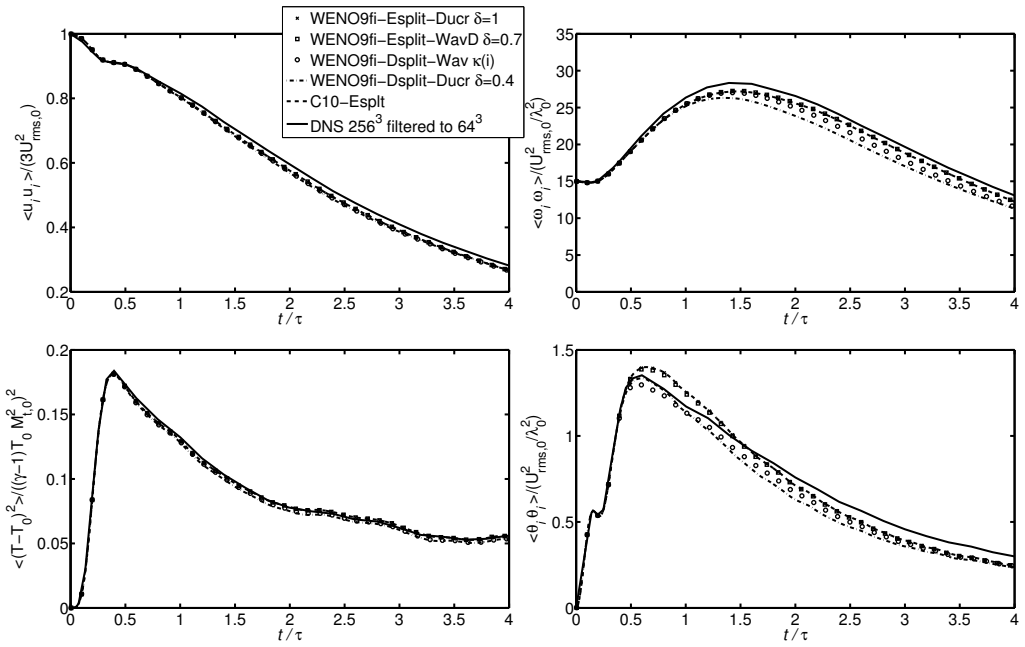

FIGURE 6. LES1 scheme comparison for the isotropic turbulence problem using a 64^3 grid: Same as Figure 5 with the results obtained using the Smagorinsky SGS model (LES1).

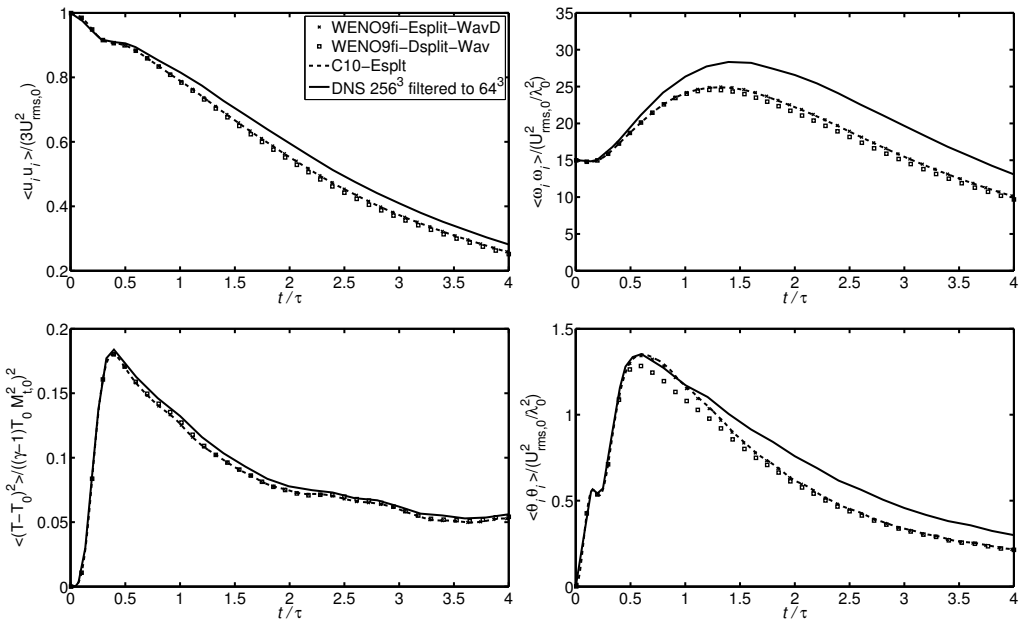

FIGURE 7. LES2 scheme comparison for the isotropic turbulence problem using a 64^3 grid: Same as Figure 5 with the results obtained using the Germano-Lilly SGS model (LES2).

cated in (9) vs. setting $C_I = 0$ are similar. This behavior might be due to the fact that the final turbulent Mach number for the considered time integration is $M_t = 0.29$. There is, however, a slightly different result by the LES2 on some of the computed flow quantities by using the non-zero C_I. Only results using $C_I = 0$ have been presented in this work. Further investigations are needed on the reason why the computed result by LES1 perform better than by the LES2 model, and on the simulation behavior depending on the choice of C_I.

Acknowledgments

The support of the DOE/SciDAC SAP grant DE-AI02-06ER25796 is acknowledged. Financial support from the NASA Aerosciences/RCA program for the second author is gratefully acknowledged. Work by the fourth author was performed under the auspices of the U.S. Department of Energy at Lawrence Livermore National Laboratory under Contract DE-AC52-07NA27344.

REFERENCES

BRACHET, M., MEIRON, D., ORSZAG, S., NICKEL, B., MORF, R. & FRISCH, U. 1983 Small-scale structure of the taylorgreen vortex. *J. Fluid Mech.* **130**, 411–452.

CIMENT, M. & LEVENTHAL 1975 Higher order compact implicit sehemes for the wave equation. *Math. Comput.* **29**, 985–994.

DUCROS, F., FERRAND, V., NICOUD, F., WEBER, C., DARRACQ, D., GACHERIEU, C. & POINSOT, T. 1999 Large-eddy simulation of the shock/turbulence interaction. *J. Comput. Phys.* **152**, 517–549.

Ducros, F., Laporte, F., Soulères, T., Guinot, V., Moinat, P. & Caruelle, B. 2000 High-order fluxes for conservative skew-symmetric-like schemes in structured meshes: Application to compressible flows. *J. Comp. Phys.* **161**, 114–139.

Erlebacher, G., Hussaini, M. Y., Speziale, C. G. & Zang, T. A. 1992 Toward the large eddy simulation of compressible turbulent flows. *J. Fluid Mech.* **238**, 155–185.

Germano, M., Piomelli, U., Moin, P. & Cabot, W. 1991 A dynamic subgrid-scale eddy viscosity model. *Phys. Fluids* **3**, 1760–1765.

Hadjadj, A., Yee, H. C. & Sjögreen, B. 2012 LES of temporally evolving mixing layers by an eighth-order filter scheme. *Int. J. Numer. Methods Fluids* **70**, 1405–1427.

Johnsen, E., Larsson, J., Bhagatwala, A., Cabot, W., Moin, P., Olson, B., Rawat, P., Shankar, S., Sjögreen, B., Yee, H., Zhong, X. & Lele, S. 2010 Assessment of high-resolution methods for numerical simulations of compressible turbulence with shock waves. *J. Comput. Phys.* **229**, 1213–1237.

Kotov, D., Yee, H. C., Hadjadj, A., Wray, A. & Sjögreen, B. 2014 High order numerical methods for les of turbulent flows with shocks. In *Proceedings of the ICCFD8*.

Kotov, D., Yee, H. C. & Sjögreen, B. 2013 Performance of improved high-order filter schemes for turbulent flows with shocks. In *Proceedings of the ASTRONUM-2013*.

Lee, S., Lele, S. & Moin, P. 1991 Eddy shocklets in decaying compressible turbulence. *Phys. Fluids* **3**, 657–664.

Lilly, D. K. 1992 A proposed modification of the Germano subgrid-scale closure method. *Phys. Fluids* **4**, 633–635.

Lo, S.-C., Blaisdell, G. & Lyrintzis, A. 2010 High-order shock capturing schemes for turbulence calculations. *J. Num. Meth. Fluids* **62** (5), 473–498.

Lombardini, M., Hill, D. J., Pullin, D. I. & Meiron, D. I. 2011 Atwood ratio dependence of richtmyermeshkov flows under reshock conditions using large-eddy simulations. *J. Fluid Mech.* **670**, 439–480.

Olsson, P. 1995 Summation by parts, projections, and stability. I. *Math. Comput.* **64**, 1035–1065.

Olsson, P. & Oliger, J. 1994 *Energy and maximum norm estimates for nonlinear conservation laws.* Technical Report no. 94.01, RIACS.

Sandham, N. D., Li, Q. & Yee, H. C. 2002 Entropy splitting for high-order numerical simulation of compressible turbulence. *J. Comp. Phys.* **178**, 307–322.

Sjögreen, B. & Yee, H. C. 2004 Multiresolution wavelet based adaptive numerical dissipation control for shock-turbulence computation. *J. Sci. Comput.* **20**, 211–255.

Sjögreen, B. & Yee, H. C. 2007 On tenth-order central spatial schemes. In *Proceedings of the Turbulence and Shear Flow Phenomena 5 (TSFP-5)*.

Sjögreen, B. & Yee, H. C. 2009 On skew-symmetric splitting and entropy conservation schemes for the euler equations. In *Proc. of the 8th Euro. Conf. on Numerical Mathematics & Advanced Applications (ENUMATH 2009)*.

Sjögreen, B., Yee, H. C. & Vinokur, M. 2014 On high order finite-difference metric discretizations satisfying GCL on moving and deforming grids. *J. Comput. Phys.* **265**, 211–220.

Taylor, G. & Green, A. 1937 Mechanism of the production of small eddies from large ones. *Proc. R. Soc. London A* **158**, 499–521.

Touber, E. & Sandham, N. 2011 Comparison of three large-eddy simulations of shock-induced turbulent separation bubbles. *Shock Waves* **19** (6), 469–478.

Yee, H. & Sjögreen, B. 2002 *Designing adaptive low dissipative high order schemes for long-time integrations.* In: Turbulent Flow Computation, (ed. D. D. . B. Geurts). Kluwer Academic.

Yee, H. C., Sandham, N. & Djomehri, M. 1999 Low dissipative high order shock-capturing methods using characteristic-based filters. *J. Comput. Phys.* **150**, 199–238.

Yee, H. C. & Sjögreen, B. 2007 Development of low dissipative high order filter schemes for multiscale Navier-Stokes/MHD systems. *J. Comput. Phys.* **225**, 910–934.

Yee, H. C. & Sjögreen, B. 2007 Simulation of Richtmyer-Meshkov instability by sixth-order filter methods. *Shock Waves* **17**, 185–193.

Yee, H. C. & Sjögreen, B. 2010 High order filter methods for wide range of compressible flow speeds. In *Proc. of ICOSAHOM 09*.

Yee, H. C., Sjögreen, B. & Hadjadj, A. 2011 Comparative study of high order schemes for LES of temporal-evolving mixing layers. In *Proc. of ASTRONUM-2010*

Yee, H. C., Sjögreen, B. & Hadjadj, A. 2012 Comparative study of three high order schemes for LES of temporally evolving mixing layers. *Commun. Comput. Phys.* **12**, 1603–1622.

Yee, H. C., Vinokur, M. & Djomehri, M. 2000 Entropy splitting and numerical dissipation. *J. Comput. Phys.* **162**, 33–81.